© 2021. Published by The Company of Biologists Ltd | Journal of Cell Science (2021) 134, jcs258459. doi:10.1242/jcs.258459

RESEARCH ARTICLE

Vacuolar H^+-ATPase dysfunction rescues intralumenal vesicle cargo sorting in yeast lacking $PI(3,5)P_2$ or Doa4

Zachary N. Wilson*, Dalton Buysse, Matt West, Daniel Ahrens and Greg Odorizzi‡

ABSTRACT

Endosomes undergo a maturation process highlighted by a reduction in lumenal pH, a conversion of surface markers that prime endosome–lysosome fusion and the sequestration of ubiquitylated transmembrane protein cargos within intralumenal vesicles (ILVs). We investigated ILV cargo sorting in mutant strains of the budding yeast *Saccharomyces cerevisiae* that are deficient for either the lysosomal/vacuolar signaling lipid $PI(3,5)P_2$ or the Doa4 ubiquitin hydrolase that deubiquitylates ILV cargos. Disruption of $PI(3,5)P_2$ synthesis or Doa4 function causes a defect in sorting of a subset of ILV cargos. We show that these cargo-sorting defects are suppressed by mutations that disrupt Vph1, a subunit of vacuolar H^+-ATPase (V-ATPase) complexes that acidify late endosomes and vacuoles. We further show that Vph1 dysfunction increases endosome abundance, and disrupts vacuolar localization of Ypt7 and Vps41, two crucial mediators of endosome–vacuole fusion. Because V-ATPase inhibition attenuates this fusion and rescues the ILV cargo-sorting defects in yeast that lack $PI(3,5)P_2$ or Doa4 activity, our results suggest that the V-ATPase has a role in coordinating ILV cargo sorting with the membrane fusion machinery.

This article has an associated First Person interview with the first author of the paper.

KEY WORDS: Endosomes, Intralumenal vesicles, V-ATPase, Membrane fusion

INTRODUCTION

Endosomes sort proteins that traffic between the Golgi complex and plasma membrane, and they fuse with lysosomes to deliver hydrolases, transporters and other resident proteins that are key to lysosomal function. Endosomes trafficking toward lysosomes undergo a maturation process, the hallmarks of which include a decrease in lumenal pH, and the acquisition and activation of Rab7, a GTPase that regulates membrane fusion between late endosomes and lysosomes (Huotari and Helenius, 2011). As they mature, endosomes also accumulate intralumenal vesicles (ILVs), which are delivered into the hydrolytic interior of lysosomes upon endosome–lysosome fusion (Hanson and Cashikar, 2012). The extent to which these aspects of endosome maturation are coordinated is still being resolved.

Department of Molecular Cellular and Developmental Biology, University of Colorado, Boulder, CO 80309, USA.
*Present address: Department of Biochemistry, University of Utah School of Medicine, Salt Lake City, UT 84112, USA.

‡Author for correspondence (odorizzi@colorado.edu)

Z.N.W., 0000-0003-4269-4058; D.B., 0000-0003-0218-7414; M.W., 0000-0002-4710-9252; D.A., 0000-0001-5318-741X; G.O., 0000-0002-1143-1098

Handling Editor: Mahak Sharma
Received 25 January 2021; Accepted 25 June 2021

The formation of ILVs during endosome maturation is mediated by the endosomal sorting complexes required for transport (ESCRTs). This conserved machinery also functions to select cargo proteins sorted into ILVs. Most ILV cargos that have been delivered to endosomes from the Golgi (biosynthetic cargos) or from the plasma membrane (endocytic cargos) are ubiquitylated transmembrane proteins that directly interact with ubiquitin-binding ESCRT subunits (Katzmann et al., 2001; Bilodeau et al., 2002; Alam et al., 2004). Mutations that generally disable ESCRTs in the budding yeast *Saccharomyces cerevisiae* block the formation of ILVs, which causes mislocalization of cargos to the membrane of the vacuole (the yeast lysosome) upon endosome–vacuole fusion. However, the efficiency with which endosomes fuse with vacuoles appears impaired under these conditions because ESCRT dysfunction also causes enlarged endosomes to accumulate and disables endosomal recruitment of the Rab7 effector HOPS (Rieder et al., 1996; Nickerson et al., 2006; Russell et al., 2012). These observations are consistent with coordination between ESCRT activity and the machinery that mediates fusion of endosomes and vacuoles.

ESCRT activity at endosomes depends on phosphatidylinositol 3-phosphate [PI(3)P], which binds a subset of ESCRT complexes to facilitate their recruitment to the endosomal membrane (Schu et al., 1993; Raiborg et al., 2001; Slagsvold et al., 2005). At late endosomes and vacuoles/lysosomes, PI(3)P is phosphorylated by a PI(3)P 5-kinase (Fab1 in yeast, PIKfyve in humans) to produce phosphatidylinositol 3,5-bisphosphate [$PI(3,5)P_2$] (Gary et al., 1998; Sbrissa et al., 1999). $PI(3,5)P_2$ has a conserved role in promoting fission of vacuoles/lysosomes, in part by activating the Yvc1/TRPML (also known as MCOLN1 in humans) channel that releases Ca^{2+} from the vacuole/lysosome into the cytosol (Bonangelino et al., 2002; Dong et al., 2010). $PI(3,5)P_2$ also inhibits the membrane fusion activity of vacuoles in yeast (Miner et al., 2018), though the molecular target of $PI(3,5)P_2$ in this case is unknown. Intriguingly, mutations that eliminate or severely cripple $PI(3,5)P_2$ synthesis impair the sorting of biosynthetic ubiquitylated ILV cargos but not endocytic ILV cargos or biosynthetic cargos that are sorted independently of direct ubiquitylation (Odorizzi et al., 1998; Dove et al., 2002). The same cargo-specific sorting defect occurs in yeast lacking Doa4, a ubiquitin hydrolase that deubiquitylates ILV cargos prior to their enclosure within ILVs (Katzmann et al., 2001). It is unclear if this cargo-specific sorting defect is an indirect result of dysregulated membrane trafficking dynamics or if $PI(3,5)P_2$ and Doa4 directly participate in ILV cargo sorting.

$PI(3,5)P_2$ synthesis by Fab1 in yeast is stimulated by hyperosmotic stress and cells that are deficient in Fab1 kinase activity cannot adapt to osmotic stressors, including elevated temperature (Yamamoto et al., 1995; Dove et al., 1997). This temperature-sensitive growth phenotype is suppressed by mutations that disable the function of Vph1 (Wilson et al., 2018), a subunit of the membrane-embedded V_0 domain of the vacuolar H^+-ATPase (V-ATPase) (Manolson et al., 1992). Here, we show that Vph1

Journal of Cell Science (2021) 134, jcs258459. doi:10.1242/jcs.258459

dysfunction suppresses defective sorting of ubiquitin-dependent biosynthetic cargos in yeast lacking PI(3,5)P_2 and, unexpectedly, also in yeast lacking the ubiquitin hydrolase Doa4. We further show that Vph1 dysfunction increases endosome abundance and impairs vacuolar membrane recruitment of Ypt7, which is the Rab7 ortholog that regulates vacuole membrane fusion activity. Because the ILV cargo-sorting defect in yeast that lack PI(3,5)P_2 and Doa4 activity is suppressed when V-ATPase activity is inhibited – which also attenuates endosome–vacuole fusion – we propose that the timing of this fusion event is important for efficient removal of ILV cargos from the endosomal membrane, a coordination that could be bridged through regulating the V-ATPase.

RESULTS

Vph1 dysfunction restores ILV cargo-sorting in yeast lacking the Fab1 kinase

Carboxypeptidase S (Cps1) is one of the ubiquitin-dependent biosynthetic cargos in yeast, whose sorting into ILVs at late endosomes is adversely affected when PI(3,5)P_2 synthesis is inhibited (Odorizzi et al., 1998). GFP fused to the cytosolic domain of Cps1 in wild-type yeast is predominantly present within the lumen of the vacuole (lysosome) because ILVs are delivered into the vacuole upon late endosome–vacuole fusion. In contrast, deletion of the *FAB1* gene (*fab1*Δ) causes mislocalization of GFP-Cps1 to the vacuole membrane (Fig. 1A and B; Odorizzi et al., 1998) because proteins that are not sorted into ILVs (or recycled away from endosomes) are ultimately delivered to the vacuole membrane.

We tested whether GFP-Cps1 mislocalization in *fab1*Δ cells was suppressed by deletion of the *VPH1* gene because Vph1 loss-of-function mutations suppress the temperature-sensitive growth of *fab1*Δ cells and other yeast strains that are deficient in PI(3,5)P_2 synthesis (Wilson et al., 2018). Indeed, GFP-Cps1 was correctly localized within the vacuole lumen in ∼80% of *fab1*Δ*vph1*Δ cells (Fig. 1A and B). GFP-Cps1 was also sorted correctly in *fab1*Δ cells when the wild-type *VPH1* gene was replaced with the *vph1*^{R735Q}

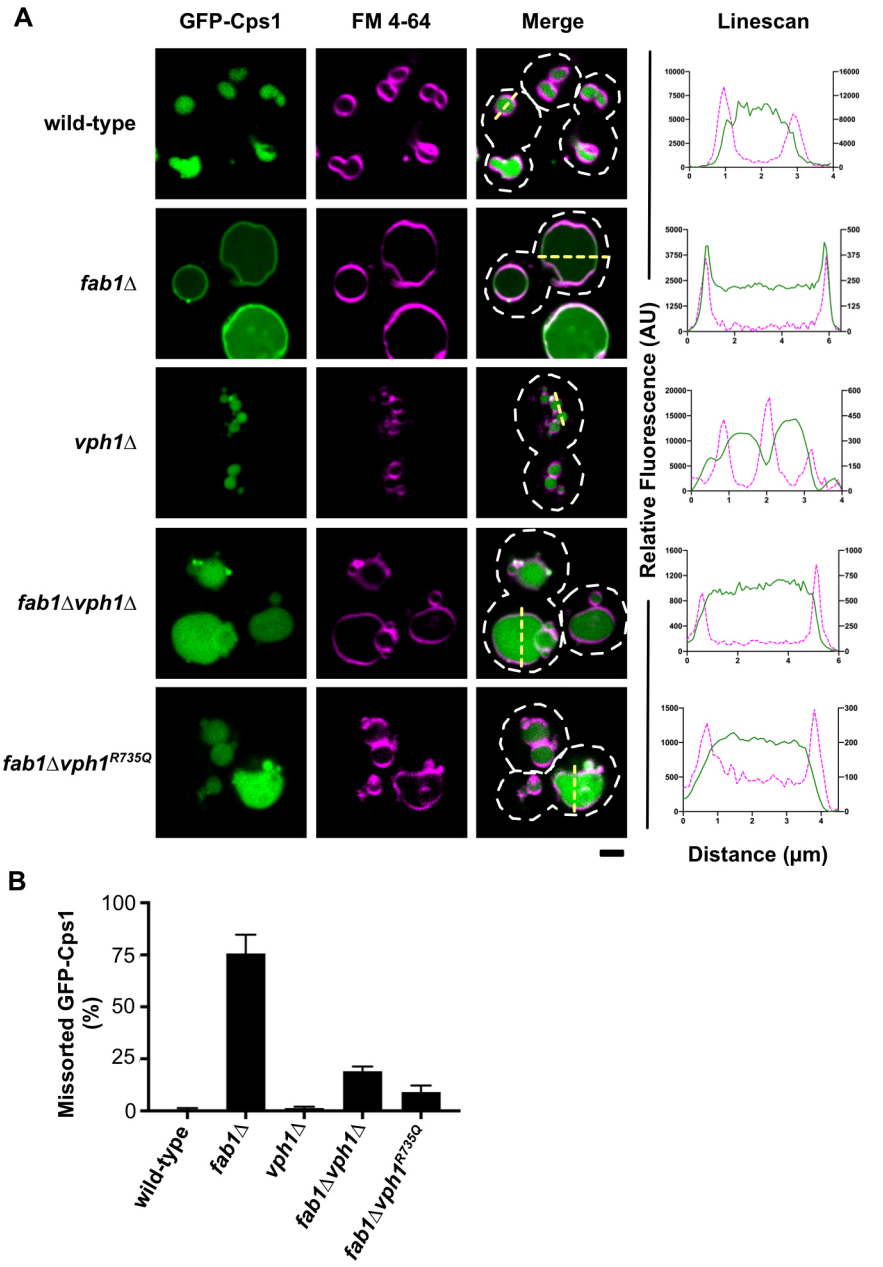

Fig. 1. Vph1 dysfunction restores ILV cargo sorting in *fab1*Δ yeast. (A) Live-cell confocal fluorescence microscopy analysis of GFP-Cps1 localization in the indicated yeast strains. GFP-Cps1 is shown in green, the vacuole membrane stained with the lipophilic fluorescent dye FM 4-64 is shown in magenta. Relative fluorescence intensities along the yellow dashed line within each merged image are plotted in the graphs on the right. White dashed lines represent cell outlines. Scale bar: 2 µm. (B) Quantification of missorted GFP-Cps1 within the strains imaged in A. Plotted is the mean amount of missorted GFP-Cps1 (in %). Error bars represent ±s.e.m. calculated from three independent experiments (n=50). GFP-Cps1 missorting was determined through either a visual or a line scan assessment of GFP-Cps1 accumulation on the vacuole membrane stained with FM 4-64.

Journal of Cell Science (2021) 134, jcs258459. doi:10.1242/jcs.258459

allele (Fig. 1A and B), which has a point mutation that disrupts proton pumping without affecting the assembly or trafficking of the V-ATPase (Kawasaki-Nishi et al., 2001; Coonrod et al., 2013). Vph1 dysfunction, therefore, suppresses the ILV cargo-sorting defect in yeast lacking the Fab1 PI(3)P 5-kinase that synthesizes $PI(3,5)P_2$.

We have previously reported that temperature-sensitive growth of *fab1*Δ cells is also suppressed by disruption of Vnx1, a proton/cation antiporter that functionally depends on vacuolar acidification by the V-ATPase (Wilson et al., 2018). Deletion of the *VNX1* gene in *fab1*Δ cells partially suppressed GFP-Cps1 mislocalization, although not to the same extent observed in *fab1*Δ*vph1*Δ yeast cells (Fig. S1A,B). Because Vph1 dysfunction has a stronger effect in suppressing GFP-Cps1 mislocalization in *fab1*Δ cells, we further explored the relationship between V-ATPase activity and ILV cargo sorting.

V-ATPase inactivation at late endosomes and vacuoles rescues ILV cargo sorting in $PI(3,5)P_2$-deficient yeast

The V-ATPase is a multisubunit protein complex that pumps protons into the lumen of multiple secretory and endocytic compartments. In *S. cerevisiae*, each of the V-ATPase subunits is encoded by a single gene, with the exception of the 'a' subunit, which is encoded either by *VPH1* or by *STV1* (Manolson et al., 1994). The Vph1 subunit is specific to V-ATPase complexes that are targeted to late endosomes and vacuoles. V-ATPases that are retained at the Golgi and at early endosomes lack Vph1 and, instead, contain Stv1, a protein that is structurally and functionally similar to Vph1 but contains a Golgi/endosomal retention signal (Finnigan et al., 2012). Unlike *VPH1* deletion (Fig. 1A), *STV1* deletion in *fab1*Δ cells did not suppress the mislocalization of GFP-Cps1 (Fig. 2A and C), which mirrors our previous observation that the temperature-sensitive growth of *fab1*Δ yeast is suppressed by deletion of *VPH1* but not *STV1* (Wilson et al., 2018).

Fab1 function requires its assembly into a multiprotein complex that is scaffolded by the Vac14 protein (Jin et al., 2008); thus, in the absence of Vac14, yeast cells synthesize low levels of $PI(3,5)P_2$ (Dove et al., 2002) but still present similar, albeit less drastic, phenotypes compared with those observed in *fab1*Δ yeast cells. We examined *vac14*Δ cells to test whether V-ATPase inactivation suppresses the ILV cargo-sorting defect caused by $PI(3,5)P_2$ deficiency in a way that is independent of Fab1 genetic dysfunction. Like *fab1*Δ cells, *vac14*Δ cells mislocalize GFP-Cps1 to the vacuole membrane, and this mislocalization was suppressed by deletion of the *VPH1* gene (Fig. 2B and C). We observed similar results in yeast cells lacking the Vac7 protein, which co-assembles into the PI(3)P 5-kinase complex to stimulate Fab1 activity (Fig. 2B and C). V-ATPase inactivation at late endosomes and vacuoles, therefore, suppresses the ILV cargo-sorting defect that is generally caused by $PI(3,5)P_2$ deficiency in yeast.

Vph1 dysfunction impairs late endosome–vacuole fusion

We explored the effect that Vph1 dysfunction has on endosomal morphology by using thin-section transmission electron microscopy (TEM). Late endosomes are easily identified by TEM as multivesicular bodies (MVBs), which are spherical organelles that contain multiple ILVs of 25–30 nm in diameter. In an evaluation of 100 wild-type yeast cell sections, we observed 0.28 MVBs per cell section, with an average of 9–10 ILVs per MVB, matching our earlier observations (Fig. 3A-C; Russell et al., 2012). As described previously (Yamamoto et al., 1995), we observed greatly enlarged vacuoles in *fab1*Δ cells (Fig. 3A), which can be attributed to a role for $PI(3,5)P_2$ synthesis in regulating vacuolar membrane dynamics and osmotic homeostasis (Gary et al., 1998; Wilson et al., 2018). Despite the ILV cargo-sorting defects observed in *fab1*Δ cells, the MVBs in this strain were morphologically similar to MVBs in wild-type yeast in terms of their appearance (Fig. 3A and B), abundance (Fig. 3C) and mean number of ILVs (Fig. 3D). In addition to confirming that ILV budding occurs in yeast lacking Fab1 kinase function – as inferred in prior studies (Gary et al., 1998; Odorizzi et al., 1998; Dove et al., 2002) – these results highlight a disconnect between cargo sorting and ILV formation in *fab1*Δ cells.

In line with the multitude of reports documenting that *vph1*Δ cells are impaired in homotypic vacuole fusion (Bayer et al., 2003; Coonrod et al., 2013; Desfougères et al., 2016), we observed that *vph1*Δ and *fab1*Δ*vph1*Δ cells contained fragmented vacuoles, with >2-fold increase in vacuoles observed per cell section in each of these mutant strains compared to wild-type yeast (Fig. 3A and C). As seen previously in yeast strains that lack V-ATPase activity (Keuenhof et al., 2021), we observed that the vacuoles in *vph1*Δ cells are electron translucent, probably due to a defect in vacuolar storage of polyphosphates that complex with electron-dense cations (Docampo and Huang, 2016). In addition to their increased number of vacuoles, *vph1*Δ and *fab1*Δ*vph1*Δ cells exhibited an almost 2-fold increase in the number of MVBs (relative to wild-type), with 0.6 and 0.45 MVBs per cell section, respectively (Fig. 3C). Furthermore, MVBs were noticeably larger in *vph1*Δ and *fab1*Δ*vph1*Δ cells, and both mutant strains showed a 20–40% increase in the mean number of ILVs per MVB (Fig. 3B and D). This boost in the abundance and size of MVBs suggests that endosome fusion with the vacuole is impaired by Vph1 dysfunction. Supporting this interpretation, we observed an increase in vacuole and MVB abundance upon deletion of the gene encoding Ypt7 (Fig. 3B and C), a Rab7 GTPase ortholog in yeast that recruits the HOPS membrane tethering complex to promote late endosome–vacuole fusion and homotypic vacuole fusion (Haas et al., 1995; Seals et al., 2000).

Vph1 dysfunction impairs Ypt7 localization to vacuole membranes

The increased abundance and size of late endosomes/MVBs that we observed in *vph1*Δ cells (Fig. 3) prompted us to investigate the extent to which Vph1 dysfunction affects the machinery involved in late endosome–vacuole fusion. GFP fused to the GTPase Ypt7 that regulates this fusion step was predominantly seen at vacuole membranes in wild-type yeast but weakly localized to vacuole membranes in *vph1*Δ cells; instead, it appeared dispersed in this mutant strain (Fig. 4A and D). We observed a similar disruption in the localization of Vps41, a subunit of the HOPS membrane-tethering complex that functions as an effector of Ypt7 (Seals et al., 2000). GFP-Vps41 predominantly localized to vacuole membranes in wild-type yeast but was diffusely distributed in *vph1*Δ cells (Fig. 4B and D). In contrast, we found that Vph1 dysfunction had no apparent effect on the punctate localization of the Rab5 GTPase ortholog Vps21 that regulates fusion at early endosomes (Fig. 4C). Thus, the loss of endolysosomal V-ATPase function disrupts localization of the Ypt7 Rab GTPase and HOPS membrane-tethering machinery that facilitates late endosome–vacuole fusion.

Vph1 dysfunction rescues ILV cargo sorting in yeast lacking the Doa4 ubiquitin hydrolase

Doa4 is the ubiquitin hydrolase that deubiquitylates cargos when they are sorted into ILVs (Dupré and Haguenauer-Tsapis, 2001; Katzmann et al., 2001; Losko et al., 2001). Similar to *fab1*Δ cells,

Journal of Cell Science (2021) 134, jcs258459. doi:10.1242/jcs.258459

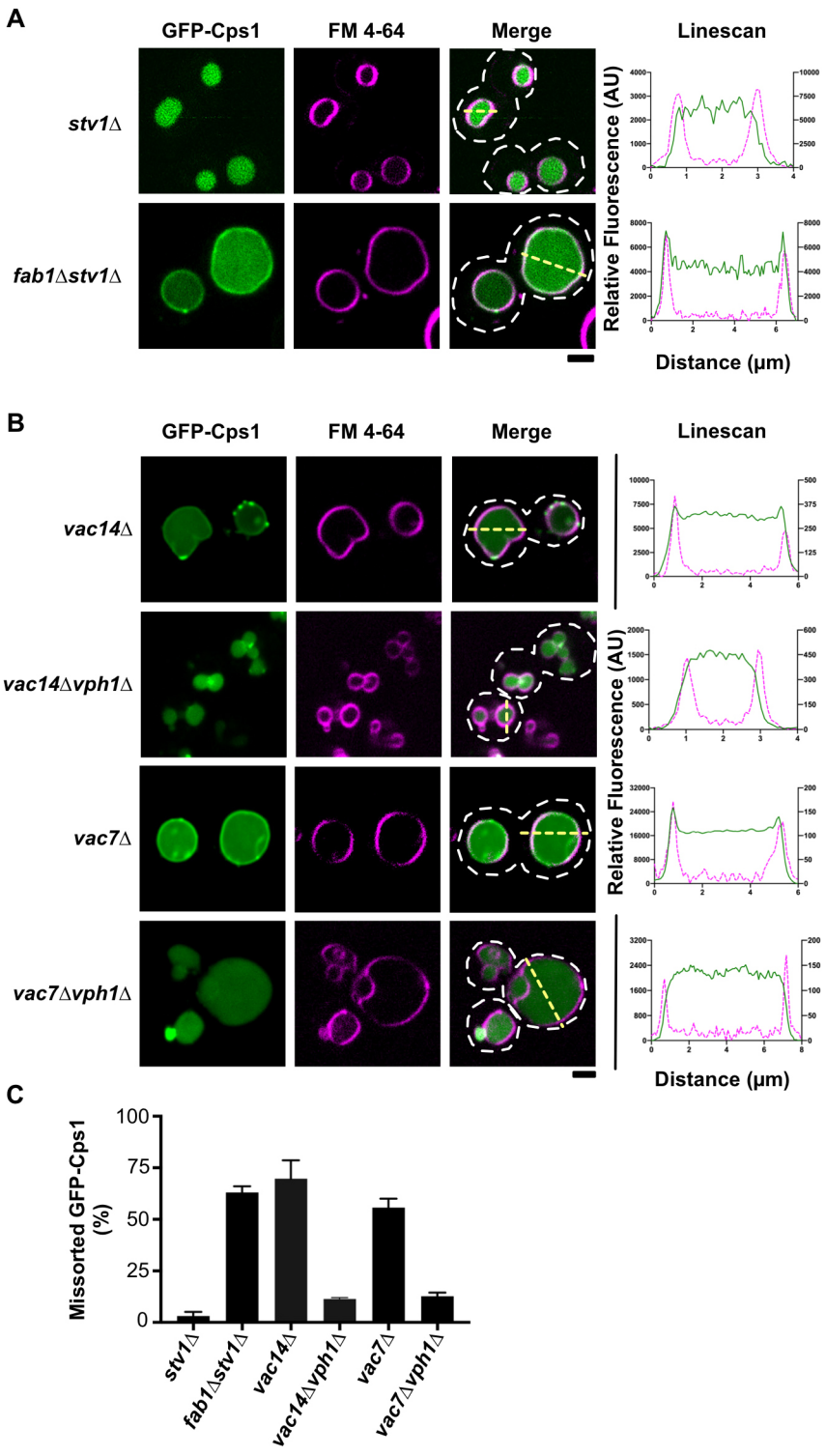

Fig. 2. V-ATPase inactivation at late endosomes and vacuoles rescues ILV cargo sorting in PI(3,5)P_2-deficient yeast. (A,B) Live-cell confocal fluorescence microscopy analysis of GFP-Cps1 localization (green) in the indicated yeast strains, the vacuole membrane was stained with FM 4-64 (magenta). Relative fluorescence intensities along the yellow dashed line within each merged image are plotted in the graphs on the right. White dashed lines represent cell outlines. Scale bars: 2 µm. (C) Quantification of missorted GFP-Cps1 within the strains imaged in A and B. Plotted is the mean amount of missorted GFP-Cps1 (in %). Error bars represent ±s.e.m. calculated from three independent experiments (*n*=50). GFP-Cps1 missorting was determined through either a visual or a line scan assessment of GFP-Cps1 accumulation on the vacuole membrane stained with FM 4-64.

*doa4*Δ cells exhibit temperature-sensitive growth and are selectively defective in the sorting of ubiquitin-dependent biosynthetic ILV cargos (Reggiori and Pelham, 2001). Also like *fab1*Δ cells, *doa4*Δ cells contain MVBs that are morphologically similar to MVBs in wild-type yeast in terms of their appearance (Fig. 3A and B), abundance (Fig. 3C) and mean number of ILVs (Fig. 3D) (Richter et al., 2007). Because of the similarities in endosomal morphologies and ILV cargo-missorting phenotypes observed in *fab1*Δ and *doa4*Δ cells, we examined whether Vph1 disruption can rescue the ILV cargo-sorting defect in the absence of Doa4 function, as seen in the case of *fab1*Δ cells (Fig. 1). Indeed, we found that *VPH1* deletion restored the sorting of GFP-Cps1 into the vacuole lumen of *doa4*Δ cells (Fig. 5A,B). Furthermore, deletion of *VPH1* in *doa4*Δ yeast appeared to disrupt vacuole fusion to the extent that had been observed in *fab1*Δ*vph1*Δ cells, as demonstrated by an increase in the total number of vacuoles per cell section (Fig. 3A,C). MVBs in *doa4*Δ*vph1*Δ yeast were also similar to those observed in *fab1*Δ*vph1*Δ cells, as they were noticeably larger and had a similar

Journal of Cell Science (2021) 134, jcs258459. doi:10.1242/jcs.258459

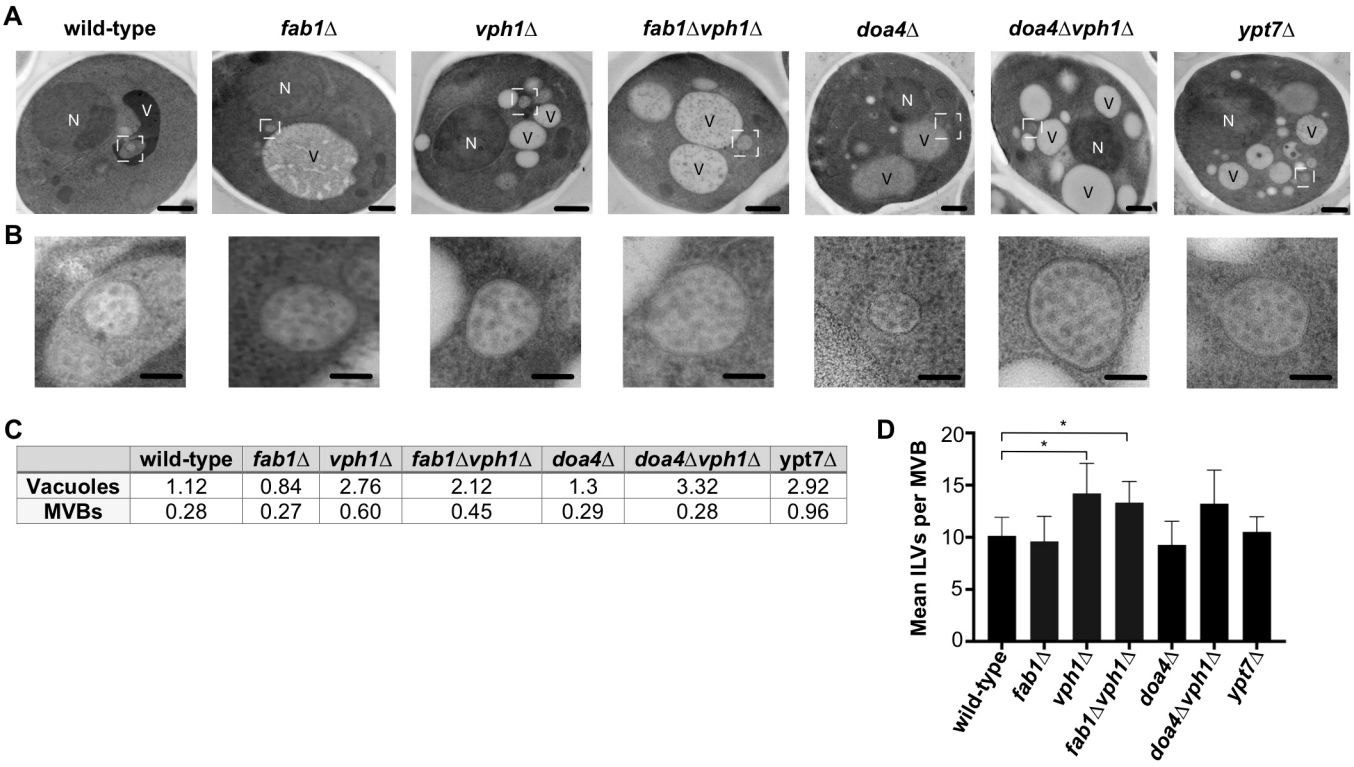

	wild-type	*fab1*Δ	*vph1*Δ	*fab1*Δ*vph1*Δ	*doa4*Δ	*doa4*Δ*vph1*Δ	ypt7Δ
Vacuoles	1.12	0.84	2.76	2.12	1.3	3.32	2.92
MVBs	0.28	0.27	0.60	0.45	0.29	0.28	0.96

Fig. 3. Vph1 dysfunction impairs late endosome–vacuole fusion. (A,B) Thin-section TEM analysis of 80-nm cell sections from the indicated yeast strains. Nuclei and some vacuoles are labeled N and V, respectively. Scale bars: 500 nm. Boxed areas in A indicate the formation of MVBs and are shown magnified in B. Scale bars: 100 nm. (C) Quantification of the number of vacuoles and MVBs observed per cell section in the strains imaged in A (n=100; 80-nm cell sections). (D) Quantification of the mean number of ILVs observed per MVB within each yeast strain. Error bars show 95% confidence intervals. Unpaired t-test with Welch's correction was used to determine statistical significance (*P<0.05).

increase in the mean number of ILVs observed per MVB (Fig. 3D). However, *VPH1* deletion did not suppress the temperature-sensitive growth of *doa4*Δ cells (Fig. 5C), presumably because Vph1 dysfunction did not restore ubiquitin homeostasis (see below).

To quantitatively assess the sorting of Cps1 into ILVs, we used the luciferase reporter of intraluminal deposition (LUCID) assay (Nickerson and Merz, 2015). LUCID is a relative dual-luciferase assay, wherein the sequestration of Cps1 into ILVs is quantitated by measuring the luminescence released by firefly luciferase (FLuc) attached to the cytosolic domain of Cps1 (FLuc-Cps1); to control for cell-to-cell variations in FLuc-Cps1 expression levels, its luminescence is compared to an internal control of cytosolic *Renilla* luciferase (RLuc) expressed from the same plasmid. Importantly, the LUCID sorting assay is sensitive to FLuc-Cps1 sequestration into ILVs and does not rely on the eventual degradation of firefly luciferase in the vacuole (Nickerson and Merz, 2015). Using the LUCID assay, we observed that both *fab1*Δ and *doa4*Δ cells showed a 2- and 3-fold increase, respectively, in the FLuc-Cps1 to RLuc ratio compared to wild-type yeast, indicating a defect in sequestering FLuc-Cps1 within the lumen of endosomes and vacuoles (Fig. 5D). Consistent with our fluorescence microscopy results, Vph1 disruption significantly reduced the FLuc-Cps1 to RLuc ratio in both *fab1*Δ and *doa4*Δ cells (Fig. 5D). Notably, the *vph1*Δ single-mutant strain showed a normal FLuc-Cps1 to RLuc ratio that was similar to the ratio in wild-type cells (Fig. 5D), indicating that a defect in vacuolar pH homeostasis is not the means by which the FLuc-Cps1 to RLuc ratio is reduced in *vph1*Δ cells. Thus, as in the case of PI(3,5)P_2-deficient yeast, the ILV cargo-sorting defect resulting from the lack of Doa4 ubiquitin hydrolase function can be corrected by dysfunctional Vph1 at late endosomes and vacuoles.

On the basis of our observations in *vph1*Δ cells, we investigated whether more substantial inhibition of endosome–vacuole fusion can also rescue the ILV cargo sorting defect of *fab1*Δ or *doa4*Δ cells. Removal of the *YPT7* gene severely fragments vacuoles, which impedes assessment of GFP-Cps1 sorting by using confocal fluorescence microscopy. Using the LUCID assay, we observed that *ypt7*Δ cells showed a 2-fold increase in the FLuc-Cps1 to RLuc ratio, similar to what we observe in *fab1*Δ yeast (Fig. 5E), indicating that either a defect in FLuc-Cps1 sorting or severe inhibition of membrane trafficking kinetics in *ypt7*Δ cells allows for more FLuc-Cps1 to be detected. Whereas removal of *YPT7* in *fab1*Δ cells further increased the FLuc-Cps1 to RLuc ratio, removal of *YPT7* in *doa4*Δ yeast significantly reduced this ratio (Fig. 5E), suggesting that even a severe inhibition of endosome–vacuole fusion can aid ILV cargo-sorting in *doa4*Δ cells.

We considered the possibility that Doa4 has a functional role in PI(3,5)P_2 synthesis through Fab1 but the following findings provided no evidence to support this hypothesis. First, localization of Doa4-GFP to endosomal structures was unaffected by deletion of *FAB1* (Fig. S2A). Second, overexpression of ubiquitin, which suppresses the temperature-sensitive growth phenotype of *doa4*Δ cells (Swaminathan et al., 1999), was unable to rescue growth of the *fab1*Δ strain at elevated temperature (Fig. S2B). Third, unlike *doa4*Δ and *doa4*Δ*vph1*Δ cells, neither *fab1*Δ nor *fab1*Δ*vph1*Δ cells were depleted of unconjugated monomeric ubiquitin (Fig. S2C). Finally, GFP-Cps1 mislocalization in *doa4*Δ cells was not suppressed by expression of a hyperactive mutant *fab1* allele that constitutively

Journal of Cell Science (2021) 134, jcs258459. doi:10.1242/jcs.258459

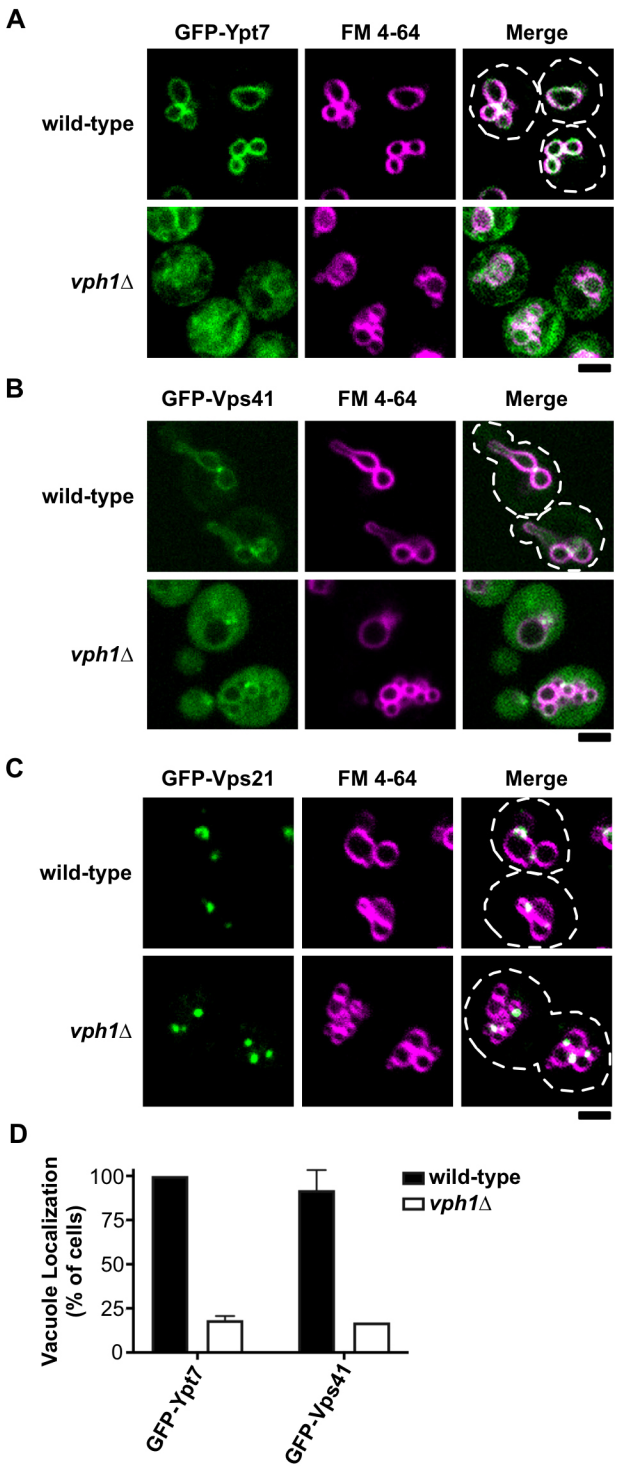

Fig. 4. Ypt7 localization to vacuole membranes is impaired in *vph1*Δ cells. (A–C) Live-cell confocal fluorescence microscopy analysis of GFP-Ypt7 (A), GFP-Vps41 (B) and GFP-Vps21 (C) localization (green) in the indicated yeast strains; the vacuole membrane was stained with the lipophilic fluorescent dye FM 4-64 (magenta). White dashed lines represent cell outlines. Scale bars: 2 µm. (D) Quantification of the vacuole localization of GFP-Ypt7 and GFP-Vps41 in wild type and *vph1Δ* strains. Plotted is the number of cells showing GFP-Ypt7 and GFP-Vps41 localized to the vacuole (in %). Error bars show +s.d. from at least two independent experiments.

produces $PI(3,5)P_2$ (Fig. S2D; Gary et al., 2002), suggesting that the ILV cargo-sorting defect observed in *doa4*Δ cells is not due to $PI(3,5)P_2$ depletion. On the basis of this set of analyses, Doa4 and Fab1 do not appear to depend on each other for function, although we cannot rule out a functional relationship observed by other means of analysis. Nevertheless, our results suggest that Doa4 and Fab1 function at a similar juncture within ILV cargo sorting, that is before the V-ATPase promotes endosome fusion with the vacuole.

DISCUSSION

We investigated the ILV cargo-sorting defect observed in *fab1*Δ yeast, which completely lack $PI(3,5)P_2$ synthesis, and in *doa4*Δ yeast, which is unable to deubiquitylate ILV cargos. We found that removal of Vph1 and, thus, vacuolar V-ATPase complexes, restored ILV cargo sorting in *fab1*Δ and *doa4*Δ yeast, an effect that appears to be due to attenuated endosome–vacuole fusion based on the increase in MVB abundance and the reduction in vacuolar localization of membrane fusion regulators in *vph1*Δ cells. These results suggest that a particular activity of Vph1-containing V-ATPases functions after $PI(3,5)P_2$ and Doa4, between the completion of ILV cargo sorting and the commencement of endosome–vacuole fusion. Therefore, $PI(3,5)P_2$ and Doa4 might have roles in coordinating ILV cargo sorting with the vacuole membrane fusion machinery at endosomes. The Cps1 cargo protein proved useful to reveal this potential relationship because this cargo, when not sorted into ILVs, accumulates on the vacuole membrane, whereas plasma membrane receptors and other cargos can undergo iterative sorting through repeated rounds of endocytosis and recycling. The lack of iterative sorting for Cps1 would explain why our steady-state cargo localization studies detected a reduction of its sorting into ILVs, although we cannot rule out the possibility that hierarchies exist in the efficiency of sorting some cargos better than others or that biosynthetic cargos are modified or processed differently than endocytic cargos.

$PI(3,5)P_2$ deficiency results in substantially enlarged vacuoles/lysosomes in both yeast and animal cells (Gary et al., 1998; Ikonomov et al., 2001), caused by defects in ion storage and the balance of membrane fission/fusion dynamics. *In-vitro* analyses demonstrated that excess $PI(3,5)P_2$ inhibits homotypic fusion of purified yeast vacuoles as well as endosomal–lysosomal fusion in mammalian cell extracts (Miner et al., 2018; Ikonomov et al., 2006). Whereas some $PI(3,5)P_2$ is also required for homotypic vacuole fusion *in vitro*, our observation that MVB abundance is similar in *fab1*Δ and wild-type cells suggests that late endosome–vacuole fusion continues unimpeded in $PI(3,5)P_2$-deficient cells. $PI(3,5)P_2$ also regulates ion export by activating endolysosomal cation channels (Dong et al., 2010), a function that might be required to allow for the removal of endosome lumenal content as ILVs are generated (Chadwick et al., 2021). However, our observation that *fab1*Δ cells contain MVBs that are morphologically similar to MVBs in wild-type yeast suggests that, in the absence of Fab1 function, ILV formation still occurs but is uncoupled from ILV cargo-sorting. Considering that V-ATPase inhibition but not removal of the monovalent cation/H^+ exchanger Vnx1 efficiently restores GFP-Cps1 sorting via the ILV pathway in *fab1*Δ yeast, we propose that, in the absence of $PI(3,5)P_2$ – a negative regulator of vacuole membrane fusion (Miner et al., 2018) – fusion between late endosomes and vacuoles aberrantly occurs prior to the completion of ILV cargo sorting.

It is possible that V-ATPase inhibition indirectly affects recovery of cargo sorting into ILVs within $PI(3,5)P_2$-deficient yeast, although this recovery might be tied to how $PI(3,5)P_2$ regulates V-ATPase activity. $PI(3,5)P_2$ interacts with Vph1 and has been shown to stabilize V-ATPase complex formation and stimulate V-ATPase activity (Li et al., 2014; Banerjee et al., 2019), a function that could

Journal of Cell Science (2021) 134, jcs258459. doi:10.1242/jcs.258459

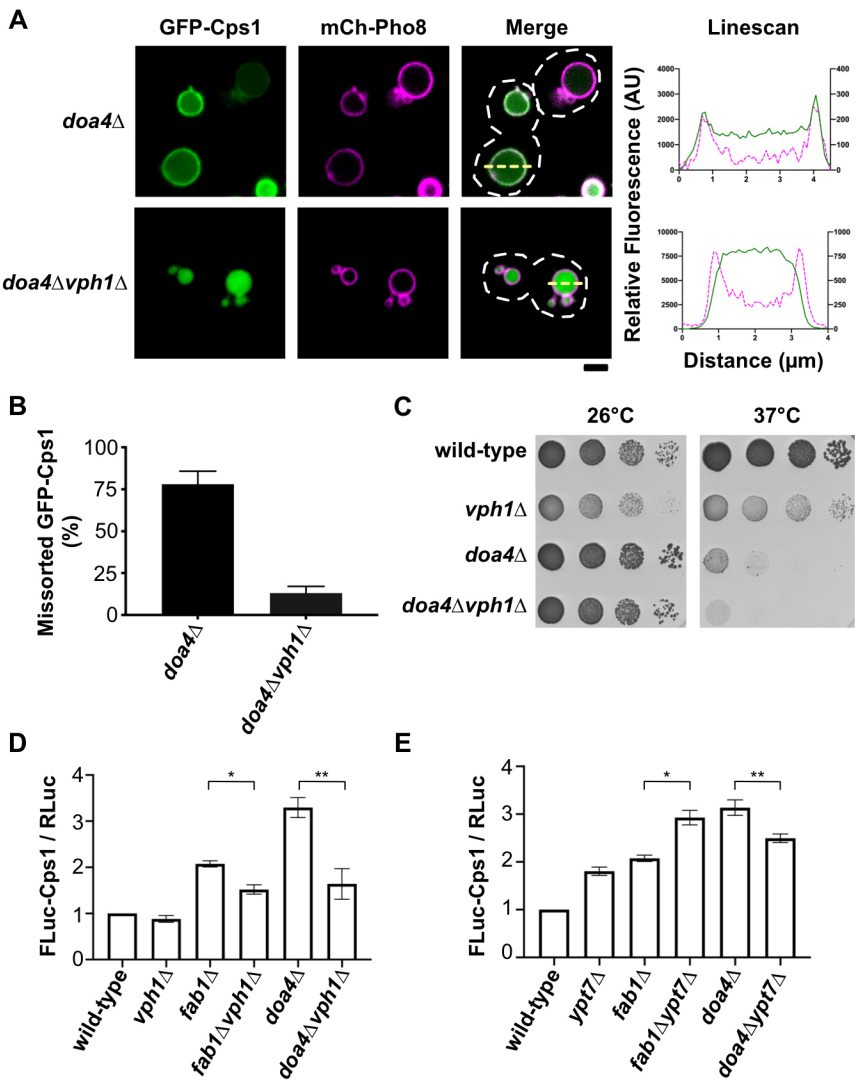

Fig. 5. Vph1 dysfunction restores ILV cargo sorting in *doa4*Δ yeast. (A) GFP-Cps1 localization (green) in the indicated yeast strains. The vacuole membrane is identified by co-expression of mCherry-Pho8 (mCh-Pho8, magenta). Relative fluorescence intensities along the yellow dashed line within each merged image are plotted in the graphs on the right. White dashed lines represent cell outlines. Scale bar: 2 µm. (B) Quantification of missorted GFP-Cps1 within the strains imaged in A. Plotted is the mean amount of missorted GFP-Cps1 (in %). Error bars represent ±s.e.m. calculated from three independent experiments (n=50). GFP-Cps1 missorting was determined through either a visual or a line scan assessment of GFP-Cps1 accumulation on the vacuole membrane. (C) Plate-spotting assays of the indicated yeast strains grown on rich (YPD) agar medium at 26°C or 37°C for 3 days, showing relative rates of yeast replication. (D,E) Quantification of missorted FLuc-Cps1 by assessing its luminescence in a LUCID assay within the indicated strains. FLuc-Cps1 to RLuc luminescence ratios were normalized to that of wild-type strain. A low FLuc-Cps1 to RLuc ratio (FLuc-Cps1 / RLuc) indicates sequestration of FLuc-Cps1 inside endosomes or vacuoles. Error bars represent ±s.e.m. calculated from three independent experiments with three technical replicates (*P<0.05, **P<0.01).

counteract the proposed role of the V-ATPase V_0 domain to support membrane fusion. To regulate membrane fusion events, free V-ATPase V_0 domains – i.e. those not bound to the V_1 domain – have been shown to interact with SNARE proteins and other free V-ATPase V_0 domains through trans-complex formation to facilitate the generation of a fusion pore (Peters et al., 2001; Strasser et al., 2011). Thus, to stabilize V-ATPase complex formation in the absence of PI(3,5)P_2, additional free V-ATPase V_0 domains may be available to promote aberrant endosome–vacuole fusion. This role of the V_0 domain in membrane fusion is dependent on Vph1 in yeast and on orthologous isoforms in animal cells (Bayer et al., 2003; Hiesinger et al., 2005; Peri and Nüsslein-Volhard, 2008). Unexpectedly, we show that Vph1 is required for vacuolar localization of the Ypt7 Rab GTPase, an essential controller of vacuole membrane fusion (Stroupe et al., 2009). Studies using mammalian cells (described below) demonstrated that the V-ATPase can directly recruit small GTPase proteins or their cognate GDP/GTP exchange factors (GEFs) to endosome or lysosome membranes. Intriguingly, different isoforms of Vph1 orthologs are involved in this recruitment. For example, the early endosome-specific isoform a2 (ATP6V0A2) subunit of the V_0 domain recruits ARNO, the GEF of the small GTPase Arf6, to regulate endocytic trafficking in kidney proximal tubule epithelial cells (Hurtado-Lurenzo et al., 2006). Similarly, isoform a3 subunit of the V_0 domain (TCIRG1), which targets V-ATPases to the plasma membrane in osteoclasts, was shown to function directly in the recruitment of Rab7 to secretory lysosomes, which is important for V-ATPase trafficking to the plasma membrane in these cells and for bone resorption (Matsumoto et al., 2018). The nature of the interaction between the V-ATPase and Ypt7 in yeast remains to be determined but might be part of a mechanism to regulate membrane fusion events, endosome maturation and/or maintain vacuole identity.

Similar to PI(3,5)P_2, Doa4 functions at late endosomes and is recruited through its interactions with the ESCRT-III complex that mediates budding of ILVs (Luhtala and Odorizzi, 2004; Richter et al., 2013; Buysse et al., 2020). At late endosomes, Doa4 recycles ubiquitin from ILV cargos prior to ILV budding from the endosome limiting membrane. Potentially as a means to control the timing of ILV budding, Doa4 negatively regulates the ILV membrane scission step that is catalyzed by ESCRT-III (Johnson et al., 2017; Buysse et al., 2020). On the basis of our observations, it is possible that Doa4 also delays ILV scission to support the efficient sequestration of cargo proteins. Without this regulation, some ILV cargos are sorted incorrectly, an inefficiency that can be rectified by attenuating (*vph1*Δ) or severely inhibiting (*ypt7*Δ) endosome–vacuole fusion. Because Doa4 negatively regulates ILV membrane scission to ensure ubiquitin recycling, it is reasonable to hypothesize that Doa4 also negatively regulates endosome–vacuole fusion; we

will examine this in future studies. Collectively, our results imply that Doa4 and PI(3,5)P_2 function prior to the V-ATPase at a similar nexus between ILV cargo sorting and endosome–vacuole fusion.

MATERIALS AND METHODS

Yeast strains, media and growth conditions

All yeast strains and plasmids used in this study are listed in Tables S1 and S2. Genomic disruptions in yeast were constructed by using homologous recombination of integration cassettes, as described by Longtine et al. (1998) or Gauss et al. (2005). Each yeast strain was authenticated and tested for contamination prior to experimental analysis. Yeast cells were grown at 26°C (unless stated otherwise) in YPD medium (1% yeast extract, 2% peptone, 2% dextrose) or minimal synthetic medium (YNB) lacking the appropriate nutrient for selection. Yeast strains containing *URA3* or *TRP1* plasmids were grown in YNB-Ura or YNB-Trp supplemented with 0.10% (w/v) casamino acids. For plate-spotting assays, liquid cultures of yeast cells were grown to mid-log phase (0.5 OD_{600} unit per ml), adjusted to 1 OD_{600} unit per ml, serially diluted 10-fold and 5 µl of each dilution of cells was spotted onto agar growth medium.

Fluorescence microscopy

Yeast cells were labeled with FM 4-64 (Life Technologies, Carlsbad, CA) following a pulse-chase procedure that has been previously described (Wilson et al., 2018). Briefly, 1 ml of mid-log-phase cells were suspended in YPD medium containing 1.6 µM FM 4-64 for 20 min at 30°C, then placed in 5 ml of YPD medium at 26°C for a 90 min chase period in the absence of FM 4-64 prior to microscopy. Subsequently, cells were placed in a small volume of minimal synthetic medium containing all required nutrients (YNB-Complete). Samples were randomized and then subjected to blind analysis by confocal fluorescence microscopy. GFP-Cps1 missorting was determined visually by assessing the accumulation of GFP-Cps1 colocalizing with the FM 4-64 dye that stains the vacuole membrane or through a line scan analysis showing peak fluorescence intensity that aligns with the fluorescence intensity peaks of the FM 4-64 dye. Representative line scan analyses are shown for all GFP-Cps1 images. Confocal fluorescence microscopy was performed using an inverted fluorescence microscope (TE2000-U; Nikon, Melville, NY) equipped with a 100×/ numerical aperture 1.4 oil objective and a Yokogawa spinning disk confocal system (CSU-Xm2; Nikon). Images were taken using a Photometrics (Tucson, AZ) Cascade II EM-CCD camera, acquired with Metamorph version 7.0 software (MDS Analytical Technologies, Sunnyvale, CA) and analyzed using either ImageJ software (National Institutes of Health, Bethesda, MD) or Photoshop CS5 (Adobe Systems, San Jose, CA).

Transmission electron microscopy

Thin-section transmission electron microscopy (TEM) was performed as previously described by Richter et al. (2013). Yeast cultures were grown to log-phase at 26°C, transferred to aluminum planchettes and high-pressure frozen in a Wohlwend Compact 02 High Pressure Freezer. Samples subsequently underwent freeze-substitution in 0.1% uranyl acetate and 0.25% glutaraldehyde within anhydrous acetone by using a Leica AFS (Automated Freeze Substitution, Vienna, Austria) system. During the AFS procedure, samples were washed with pure acetone and embedded in Lowicryl HM20 resin (Polysciences, Warrington, PA). A Leica Ultra-Microtome was used to cut serial thin sections of 80 nm, which were then collected onto 1% formvar films adhered to rhodium-plated copper grids (Electron Microscopy Sciences). A Phillips CM10 (Mahwah, NJ) transmission electron microscope was used to image sections at 80 kV. Images were processed using ImageJ software or Photoshop CS5 and graphics/statistical analyses were performed using Graphpad Prism software.

Western blotting

Protein extracts from whole yeast cells were obtained by addition of 10% (v/v) trichloroacetic acid to liquid cultures of log-phase yeast, incubation on ice for 20 min and centrifugation at 16,100× ***g*** for 5 min at 4°C. Three times, the precipitated pellet was resuspended by sonication into ice-cold acetone and centrifuged again before being resuspended in Laemmli buffer. Glass beads (0.5-mm) were then added to each sample and the precipitate was mechanically disrupted by vortex agitation for 10 min before being boiled at 95°C. Extracts were resolved by SDS-PAGE in 4-20% acrylamide (v/v) Tris/glycine gradient gels (Bio-Rad Laboratories). Proteins were transferred to nitrocellulose membranes and incubated with mouse monoclonal primary antibodies reactive against yeast Pgk1 (catalog no. 22C5D8; ThermoFisher Scientific) or Ubiquitin (catalog no. 14-6078-82; ThermoFisher Scientific). Primary antibodies were validated by western blot analysis of a deletion strain extract (Pgk1) or of a wild-type yeast strain overexpressing ubiquitin from a high-copy-number plasmid. Primary antibodies were detected by using goat anti-mouse HRP-conjugated secondary antibody (catalog no. sc-2005; Santa Cruz Biotechnology) that allowed for chemiluminescent detection by film exposure.

LUCID assay

Quantitative analysis of firefly luciferase-Cps1 (FLuc-Cps1) sorting into MVBs by using the LUCiferase reporter of Intraluminal Deposition (LUCID) assay was performed as described in Nickerson and Merz (2015) using a dual luciferase assay system (Promega, Madison, WI). All yeast strains analyzed were transformed with plasmid pDN316, grown to early log phase and treated with cyclohexamide (50 µg/ml) for 20 min. Cells (1.2 OD_{600} units) were passively lysed in 200 µl of 1× passive lysis buffer (PLB) from the dual luciferase assay system (buffered to pH 7 with 100 mM Tris-HCl pH 7.0) and vortexed with 0.5-mm glass beads. Firefly luciferase and *Renilla* luciferase (RLuc) were analyzed sequentially using a SpectraMax M5 microplate reader (Molecular Devices, Sunnyvale, CA). To determine the relative sorting of FLuc-Cps1, the signal from firefly luciferase was normalized to the signal from *Renilla* luciferase. The FLuc-Cps1 to RLuc ratios in all yeast strains were normalized to the isogenic SEY6210 wild-type yeast strain. Graphing and statistical analyses were performed using Graphpad Prism software.

Acknowledgements

We thank Alex Merz (University of Washington) and Tom Stevens (University of Oregon) for plasmids and/or yeast strains.

Competing interests

The authors declare no competing or financial interests.

Author contributions

Conceptualization: Z.N.W., G.O.; Methodology: Z.N.W., M.W.; Validation: Z.N.W., D.B., M.W.; Formal analysis: Z.N.W., D.B., M.W.; Investigation: Z.N.W., D.B., M.W.; Resources: G.O.; Data curation: Z.N.W., D.B., M.W., D.A.; Writing - original draft: Z.N.W.; Writing - review & editing: Z.N.W., G.O.; Visualization: Z.N.W., M.W.; Supervision: G.O.; Project administration: G.O.; Funding acquisition: G.O.

Funding

This work was supported by a grant from the National Institutes of Health/National Institute of General Medical Sciences to G.O. (grant no. GM111335) and by National Science Foundation GRFP (grant no. DGE-1144083) to Z.W. Deposited in PMC for release after 12 months.

Peer review history

The peer review history is available online at https://journals.biologists.com/jcs/article-lookup/doi/10.1242/jcs.258459

References

Alam, S. L., Sun, J., Payne, M., Welch, B. D., Blake, B. K., Davis, D. R., Meyer, H. H., Emr, S. D. and Sundquist, W. I. (2004). Ubiquitin interactions of NZF zinc fingers. *EMBO J.* **23**, 1411-1421. doi:10.1038/sj.emboj.7600114

Banerjee, S., Clapp, K., Tarsio, M. and Kane, P. M. (2019). Interaction of the late endo-lysosomal lipid PI(3,5)P2 with the Vph1 isoform of yeast V-ATPase increases its activity and cellular stress tolerance. *J. Biol. Chem.* **294**, 9161-9171.

Bayer, M. J., Reese, C., Bühler, S., Peters, C. and Mayer, A. (2003). Vacuole membrane fusion. *J. Cell Biol.* **162**, 211-222. doi:10.1083/jcb.200212004

Bilodeau, P. S., Urbanowski, J. L., Winistorfer, S. C. and Piper, R. C. (2002). The Vps27p–Hse1p complex binds ubiquitin and mediates endosomal protein sorting. *Nat. Cell Biol.* **4**, 534-539. doi:10.1038/ncb815

Bonangelino, C. J., Nau, J. J., Duex, J. E., Brinkman, M., Wurmser, A. E., Gary, J. D., Emr, S. D. and Weisman, L. S. (2002). Osmotic stress–induced increase of phosphatidylinositol 3,5-bisphosphate requires Vac14p, an activator of the lipid kinase Fab1p. *J. Cell Biol.* **156**, 1015-1028. doi:10.1083/jcb.200201002

Buysse, D., Pfitzner, A.-K., West, M., Roux, A. and Odorizzi, G. (2020). The ubiquitin hydrolase Doa4 directly binds Snf7 to inhibit recruitment of ESCRT-III remodeling factors in S. cerevisiae. *J. Cell Sci.* **133**, jcs241455. doi:10.1242/jcs.241455

Chadwick, S. R., Grinstein, S. and Freeman, S. A. (2021). From the inside out: Ion fluxes at the centre of endocytic traffic. *Curr. Opin. Cell Biol.* **71**, 77-86. doi:10.1016/j.ceb.2021.02.006

Coonrod, E. M., Graham, L. A., Carpp, L. N., Carr, T. M., Stirrat, L., Bowers, K., Bryant, N. J. and Stevens, T. H. (2013). Homotypic vacuole fusion in yeast requires organelle acidification and not the V-ATPase membrane domain. *Dev. Cell* **27**, 462-468. doi:10.1016/j.devcel.2013.10.014

Desfougères, Y., Vavassori, S., Rompf, M., Gerasimaite, R. and Mayer, A. (2016). Organelle acidification negatively regulates vacuole membrane fusion in vivo. *Sci. Rep.* **6**, 29045. doi:10.1038/srep29045

Docampo, R. and Huang, G. (2016). Acidocalcisomes of eukaryotes. *Curr. Opin. Cell Biol.* **41**, 66-72. doi:10.1016/j.ceb.2016.04.007

Dong, X.-P., Shen, D., Wang, X., Dawson, T., Li, X., Zhang, Q., Cheng, X., Zhang, Y., Weisman, L. S., Delling, M. et al. (2010). PI(3,5)P(2) controls membrane trafficking by direct activation of mucolipin Ca(2+) release channels in the endolysosome. *Nat. Commun.* **1**, 38. doi:10.1038/ncomms1037

Dove, S. K., Cooke, F. T., Douglas, M. R., Sayers, L. G., Parker, P. J. and Michell, R. H. (1997). Osmotic stress activates phosphatidylinositol-3,5-bisphosphate synthesis. *Nature* **390**, 187-192. doi:10.1038/36613

Dove, S. K., McEwen, R. K., Mayes, A., Hughes, D. C., Beggs, J. D. and Michell, R. H. (2002). Vac14 controls PtdIns(3,5) P 2 synthesis and Fab1-dependent protein trafficking to the multivesicular body. *Curr. Biol.* **12**, 885-893. doi:10.1016/S0960-9822(02)00891-6

Dupré, S. and Haguenauer-Tsapis, R. (2001). Deubiquitination step in the endocytic pathway of yeast plasma membrane proteins: crucial role of Doa4p ubiquitin isopeptidase. *Mol. Cell. Biol.* **21**, 4482-4494. doi:10.1128/MCB.21.14.4482-4494.2001

Finnigan, G. C., Cronan, G. E., Park, H. J., Srinivasan, S., Quiocho, F. A. and Stevens, T. H. (2012). Sorting of the yeast vacuolar-type, proton- translocating ATPase enzyme complex (V-ATPase): identification of a necessary and sufficient Golgi/endosomal retention signal in Stv1p. *J. Biol. Chem.* **287**, 19487-19500. doi:10.1074/jbc.M112.343814

Gary, J. D., Wurmser, A. E., Bonangelino, C. J., Weisman, L. S. and Emr, S. D. (1998). Fab1p is essential for PtdIns(3)P 5-kinase activity and the maintenance of vacuolar size and membrane homeostasis. *J. Cell Biol.* **143**, 65-79. doi:10.1083/jcb.143.1.65

Gary, J. D., Sato, T. K., Stefan, C. J., Bonangelino, C. J., Weisman, L. S. and Emr, S. D. (2002). Regulation of Fab1 phosphatidylinositol 3-phosphate 5-kinase pathway by Vac7 protein and Fig4, a polyphosphoinositide phosphatase family member. *Mol. Biol. Cell* **13**, 1238-1251. doi:10.1091/mbc.01-10-0498

Gauss, R., Trautwein, M., Sommer, T. and Spang, A. (2005). New modules for the repeated internal and N-terminal epitope tagging of genes in *Saccharomyces cerevisiae*. *Yeast* **22**, 1-12. doi:10.1002/yea.1187

Haas, A., Scheglmann, D., Lazar, T., Gallwitz, D. and Wickner, W. (1995). The GTPase Ypt7p of *Saccharomyces cerevisiae* is required on both partner vacuoles for the homotypic fusion step of vacuole inheritance. *EMBO J.* **14**, 5258-5270. doi:10.1002/j.1460-2075.1995.tb00210.x

Hanson, P. I. and Cashikar, A. (2012). Multivesicular body morphogenesis. *Annu. Rev. Cell Dev. Biol.* **28**, 337-362. doi:10.1146/annurev-cellbio-092910-154152

Hiesinger, P. R., Fayyazuddin, A., Mehta, S. Q., Rosenmund, T., Schulze, K. L., Zhai, R. G., Verstreken, P., Cao, Y., Zhou, Y., Kunz, J. et al. (2005). The v-ATPase V 0 subunit a1 is required for a late step in synaptic vesicle exocytosis in Drosophila. *Cell* **121**, 607-620. doi:10.1016/j.cell.2005.03.012

Huotari, J. and Helenius, A. (2011). Endosome maturation. *EMBO J.* **30**, 3481-3500. doi:10.1038/emboj.2011.286

Hurtado-Lorenzo, A., Skinner, M., El Annan, J., Futai, M., Sun-Wada, G.-H., Bourgoin, S., Casanova, J., Wildeman, A., Bechoua, S., Ausiello, D. A. et al. (2006). V-ATPase interacts with ARNO and Arf6 in early endosomes and regulates the protein degradative pathway. *Nat. Cell Biol.*, **8**, 124-136. doi:10.1038/ncb1348

Ikonomov, O. C., Sbrissa, D. and Shisheva, A. (2001). Mammalian cell morphology and endocytic membrane homeostasis require enzymatically active phosphoinositide 5-kinase PIKfyve. *J. Biol. Chem.* **276**, 26141-26147. doi:10.1074/jbc.M101722200

Ikonomov, O. C., Sbrissa, D. and Shisheva, A. (2006). Localized PtdIns 3,5-P_2 synthesis to regulate early endosome dynamics and fusion. *Am. J. Physiol. Cell Physiol.* **291**, C393-C404. doi:10.1152/ajpcell.00019.2006

Jin, N., Chow, C. Y., Liu, L., Zolov, S. N., Bronson, R., Davisson, M., Petersen, J. L., Zhang, Y., Park, S., Duex, J. E. et al. (2008). VAC14 nucleates a protein complex essential for the acute interconversion of PI3P and PI(3,5)P(2) in yeast and mouse. *EMBO J.* **27**, 3221-3234. doi:10.1038/emboj.2008.248

Johnson, N., West, M. and Odorizzi, G. (2017). Regulation of yeast ESCRT-III membrane scission activity by the Doa4 ubiquitin hydrolase. *Mol. Biol. Cell* **28**, 661-672. doi:10.1091/mbc.e16-11-0761

Katzmann, D. J., Babst, M. and Emr, S. D. (2001). Ubiquitin-dependent sorting into the multivesicular body pathway requires the function of a conserved endosomal protein sorting complex, ESCRT-I. *Cell* **106**, 145-155. doi:10.1016/S0092-8674(01)00434-2

Kawasaki-Nishi, S., Bowers, K., Nishi, T., Forgac, M. and Stevens, T. H. (2001). The amino-terminal domain of the vacuolar proton-translocating ATPase a subunit controls targeting and in vivo dissociation, and the carboxyl-terminal domain affects coupling of proton transport and ATP hydrolysis. *J. Biol. Chem.* **276**, 47411-47420. doi:10.1074/jbc.M108310200

Keuenhof, K., Berglund, L. L., Schneider, K. L., Hill, S. M., Widlund, P. O., Nyström, T. and Höög, J. L. (2021). Large organellar changes occur during mild heat shock in yeast. *J. Cell Sci.* **134**, jcs258325. doi:10.1242/jcs.258325

Li, S. C., Diakov, T. T., Xu, T., Tarsio, M., Zhu, W., Couoh-Cardel, S., Weisman, L. S. and Kane, P. M. (2014). The signaling lipid PI(3,5)P_2 stabilizes V_1-V(o) sector interactions and activates the V-ATPase. *Mol. Biol. Cell* **25**, 1251-1262. doi:10.1091/mbc.e13-10-0563

Longtine, M. S., Mckenzie, A., III, Demarini, D. J., Shah, N. G., Wach, A., Brachat, A., Philippsen, P. and Pringle, J. R. (1998). Additional modules for versatile and economical PCR–based gene deletion and modification in *Saccharomyces cerevisiae*. *Yeast* **14**, 953-961. doi:10.1002/(SICI)1097-0061(199807)14:10<953::AID-YEA293>3.0.CO;2-U

Losko, S., Kopp, F., Kranz, A. and Kölling, R. (2001). Uptake of the ATP-binding cassette (ABC) transporter Ste6 into the yeast vacuole is blocked in the *doa4* mutant. *Mol. Biol. Cell* **12**, 1047-1059. doi:10.1091/mbc.12.4.1047

Luhtala, N. and Odorizzi, G. (2004). Bro1 coordinates deubiquitination in the multivesicular body pathway by recruiting Doa4 to endosomes. *J. Cell Biol.* **166**, 717-729. doi:10.1083/jcb.200403139

Manolson, M. F., Proteau, D., Preston, R. A., Stenbit, A., Roberts, B. T., Hoyt, M. A., Preuss, D., Mulholland, J., Botstein, D. and Jones, E. W. (1992). The VPH1 gene encodes a 95-kDa integral membrane polypeptide required for in vivo assembly and activity of the yeast vacuolar H(+)-ATPase. *J. Biol. Chem.* **267**, 14294-14303. doi:10.1016/S0021-9258(19)49711-1

Manolson, M. F., Wu, B., Proteau, D., Taillon, B. E., Roberts, B. T., Hoyt, M. A. and Jones, E. W. (1994). STV1 gene encodes functional homologue of 95-kDa yeast vacuolar H(+)-ATPase subunit Vph1p. *J. Biol. Chem.* **269**, 14064-14074. doi:10.1016/S0021-9258(17)36755-8

Matsumoto, N., Sekiya, M., Tohyama, K., Ishiyama-Matsuura, E., Sun-Wada, G.-H., Wada, Y., Futai, M. and Nakanishi-Matsui, M. (2018). Essential role of the a3 isoform of V-ATPase in secretory lysosome trafficking via Rab7 recruitment. *Sci. Rep.* **8**, 6701. doi:10.1038/s41598-018-24918-7

Miner, G. E., Sullivan, K. D., Guo, A., Jones, B. C., Hurst, L. R., Ellis, E. C., Starr, M. L. and Fratti, R. A. (2018). Phosphatidylinositol 3,5-bisphosphate regulates the transition between trans-SNARE complex formation and vacuole membrane fusion. *Mol. Biol. Cell* **30**, 201-208. doi:10.1091/mbc.E18-08-0505

Nickerson, D. P. and Merz, A. J. (2015). LUCID: a quantitative assay of ESCRT-mediated cargo sorting into multivesicular bodies. *Traffic* **16**, 1318-1329. doi:10.1111/tra.12331

Nickerson, D. P., West, M. and Odorizzi, G. (2006). Did2 coordinates Vps4-mediated dissociation of ESCRT-III from endosomes. *J Cell Biol.* **175**, 715-720. doi:10.1083/jcb.200606113

Odorizzi, G., Babst, M. and Emr, S. D. (1998). Fab1p PtdIns(3)P 5-kinase function essential for protein sorting in the multivesicular body. *Cell* **95**, 847-858. doi:10.1016/S0092-8674(00)81707-9

Peri, F. and Nüsslein-Volhard, C. (2008). Live imaging of neuronal degradation by microglia reveals a role for v0-ATPase a1 in phagosomal fusion in vivo. *Cell* **133**, 916-927. doi:10.1016/j.cell.2008.04.037

Peters, C., Bayer, M. J., Bühler, S., Andersen, J. S., Mann, M. and Mayer, A. (2001). Trans-complex formation by proteolipid channels in the terminal phase of membrane fusion. *Nature* **409**, 581-588. doi:10.1038/35054500

Raiborg, C., Bremnes, B., Mehlum, A., Gillooly, D. J., D'Arrigo, A., Stang, E. and Stenmark, H. (2001). FYVE and coiled-coil domains determine the specific localisation of Hrs to early endosomes. *J. Cell Sci.* **114**, 2255-2263. doi:10.1242/jcs.114.12.2255

Reggiori, F. and Pelham, H. R. B. (2001). Sorting of proteins into multivesicular bodies: ubiquitin-dependent and -independent targeting. *EMBO J.* **20**, 5176-5186. doi:10.1093/emboj/20.18.5176

Richter, C., West, M. and Odorizzi, G. (2007). Dual mechanisms specify Doa4-mediated deubiquitination at multivesicular bodies. *EMBO J.* **26**, 2454-2464. doi:10.1038/sj.emboj.7601692

Richter, C. M., West, M. and Odorizzi, G. (2013). Doa4 function in ILV budding is restricted through its interaction with the Vps20 subunit of ESCRT-III. *J. Cell Sci.* **126**, 1881-1890. doi:10.1242/jcs.122499

Rieder, S. E., Banta, L. M., Köhrer, K., McCaffery, J. M. and Emr, S. D. (1996). Multilamellar endosome-like compartment accumulates in the yeast vps28 vacuolar protein sorting mutant. *Mol. Biol. Cell* **7**, 985-999. doi:10.1091/mbc.7.6.985

Russell, M. R. G., Shideler, T., Nickerson, D. P., West, M. and Odorizzi, G. (2012). Class E compartments form in response to ESCRT dysfunction in yeast due to hyperactivity of the Vps21 Rab GTPase. *J. Cell Sci.* **125**, 5208-5220. doi:10.1242/jcs.111310

Sbrissa, D., Ikonomov, O. C. and Shisheva, A. (1999). PIKfyve, a mammalian ortholog of yeast Fab1p lipid kinase, synthesizes 5-phosphoinositides. *J. Biol. Chem.* **274**, 21589-21597. doi:10.1074/jbc.274.31.21589

Schu, P., Takegawa, K., Fry, M., Stack, J., Waterfield, M. and Emr, S. (1993). Phosphatidylinositol 3-kinase encoded by yeast VPS34 gene essential for protein sorting. *Science* **260**, 88-91. doi:10.1126/science.8385367

Seals, D. F., Eitzen, G., Margolis, N., Wickner, W. T. and Price, A. (2000). A Ypt/Rab effector complex containing the Sec1 homolog Vps33p is required for homotypic vacuole fusion. *Proc. Natl. Acad. Sci. USA* **97**, 9402-9407. doi:10.1073/pnas.97.17.9402

Slagsvold, T., Aasland, R., Hirano, S., Bache, K. G., Raiborg, C., Trambaiolo, D., Wakatsuki, S. and Stenmark, H. (2005). Eap45 in mammalian ESCRT-II binds ubiquitin via a phosphoinositide-interacting GLUE domain. *J. Biol. Chem.* **280**, 19600-19606. doi:10.1074/jbc.M501510200

Strasser, B., Iwaszkiewicz, J., Michielin, O. and Mayer, A. (2011). The V-ATPase proteolipid cylinder promotes the lipid-mixing stage of SNARE-dependent fusion of yeast vacuoles. *EMBO J.* **30**, 4126-4141. doi:10.1038/emboj.2011.335

Stroupe, C., Hickey, C. M., Mima, J., Burfeind, A. S. and Wickner, W. (2009). Minimal membrane docking requirements revealed by reconstitution of Rab GTPase-dependent membrane fusion from purified components. *Proc Natl. Acad. Sci. USA* **106**, 17626-17633. doi:10.1073/pnas.0903801106

Swaminathan, S., Amerik, A. Y. and Hochstrasser, M. (1999). The Doa4 deubiquitinating enzyme is required for ubiquitin homeostasis in yeast. *Mol. Biol. Cell* **10**, 2583-2594. doi:10.1091/mbc.10.8.2583

Wilson, Z. N., Scott, A. L., Dowell, R. D. and Odorizzi, G. (2018). PI(3,5)P2 controls vacuole potassium transport to support cellular osmoregulation. *Mol. Biol. Cell* **29**, 1718-1731. doi:10.1091/mbc.E18-01-0015

Yamamoto, A., DeWald, D. B., Boronenkov, I. V., Anderson, R. A., Emr, S. D. and Koshland, D. (1995). Novel PI(4)P 5-kinase homologue, Fab1p, essential for normal vacuole function and morphology in yeast. *Mol. Biol. Cell* **6**, 525-539. doi:10.1091/mbc.6.5.525